

88 Hours: The U.S. Geological Survey National Earthquake Information Center Response to the 11 March 2011 M_w 9.0 Tohoku Earthquake

Gavin P. Hayes,^{1,2} Paul S. Earle,¹ Harley M. Benz,¹ David J. Wald,¹ Richard W. Briggs,¹ and the USGS/NEIC Earthquake Response Team

Online material: Timeline movie

INTRODUCTION

The M 9.0 11 March 2011 Tohoku, Japan, earthquake and associated tsunami near the east coast of the island of Honshu caused tens of thousands of deaths and potentially over one trillion dollars in damage, resulting in one of the worst natural disasters ever recorded. The U.S. Geological Survey National Earthquake Information Center (USGS NEIC), through its responsibility to respond to all significant global earthquakes as part of the National Earthquake Hazards Reduction Program, quickly produced and distributed a suite of earthquake information products to inform emergency responders, the public, the media, and the academic community of the earthquake's potential impact and to provide scientific background for the interpretation of the event's tectonic context and potential for future hazard.

Here we present a timeline of the NEIC response to this devastating earthquake in the context of rapidly evolving information emanating from the global earthquake-response community. The timeline includes both internal and publicly distributed products, the relative timing of which highlights the inherent tradeoffs between the requirement to provide timely alerts and the necessity for accurate, authoritative information. The timeline also documents the iterative and evolutionary nature of the standard products produced by the NEIC and includes a behind-the-scenes look at the decisions, data, and analysis tools that drive our rapid product distribution.

THE USGS NATIONAL EARTHQUAKE INFORMATION CENTER

The NEIC operates a 24/7 service dedicated to the rapid determination of the location and size of all significant earthquakes

1. U.S. Geological Survey National Earthquake Information Center, Golden, Colorado, U.S.A.
2. Synergetics Inc., Fort Collins, Colorado, U.S.A.

worldwide and to the immediate dissemination of this information to concerned national and international agencies, scientists, critical facilities, and the general public.

Within its 24/7 operations, the NEIC is constantly staffed by at least two geophysicists who are responsible for reviewing and reporting all magnitude 5 or larger events within 20 minutes of origin time. These analysts also field incoming calls from the media and communicate with USGS research scientists and staff following a significant damaging earthquake. In addition, the computer operations at the NEIC are continuously managed by either USGS IT staff or off-hours contractors. Typically within an hour of large, damaging earthquakes like the Tohoku event, the Earthquake Hazards Program adds analyst staff to review and disseminate earthquake information products for aftershocks, while science and geographic information system (GIS) staff begin the process of compiling value-added information and content about the kinematics of rupture, regional geology, and tectonics. The USGS Communications Office also adds staff to handle inquiries.

In recent years, the NEIC's earthquake response has evolved in three significant ways. First, the number of seismic stations available for real-time global monitoring has greatly increased. At the time of the M 9.1 2004 Sumatra-Andaman Islands earthquake, the NEIC received data from approximately 350 stations in real time; today we receive data from 1,183 stations in 83 seismic networks around the world. This includes significant improvement to the Global Seismographic Network (GSN), whose unique high dynamic range capabilities, operational stability, and real-time telemetry reliability (Butler et al. 2004) make it central to our response activities. Second, the level of interagency and international cooperation has expanded beyond the sharing of waveform data to the coordination of real-time earthquake source parameters. Third, the seismic modeling and analysis tools used by the NEIC have become more sophisticated and expedient and have significantly expanded in scope. Examples of modeling and analysis advances include improved methods to estimate basic hypocentral and earthquake source parameters, rapid and robust procedures to determine magnitude, production of finite fault mod-

els, and the rapid estimation of an earthquake's impact based on potential economic losses and fatalities.

RESPONSE OF NEIC TO THE TOHOKU EARTHQUAKE SERIES

In the minutes and hours following a significant earthquake, the NEIC continually refines its estimates of the event's source parameters. At key points during this processing, public releases are issued and updates to higher-level products are triggered. The NEIC's customers are not well served by continually updating—sometimes erroneously—automatic or preliminary estimates of magnitude and location; instead we publicly release and update information when we believe it has stabilized and is considered actionable and authoritative. Standard operating procedures are in place, but every earthquake is unique and requires an understanding of the strengths and weaknesses of the algorithms and systems used to characterize it.

The NEIC does not respond to major earthquakes in isolation. In the initial stages of the response to potentially tsunamigenic earthquakes, the NEIC coordinates its magnitudes with the National Oceanic and Atmospheric Administration (NOAA) Pacific and West Coast/Alaska Tsunami Warning Centers (PTWC and WCATWC, respectively). For earthquakes near Japan, the Tsunami Warning Centers (TWCs) in turn coordinate their hypocenters and magnitudes with the Japan Meteorological Agency (JMA). Coordination introduces some challenges but provides consistent information to emergency responders and the public. It also places the burden of reconciling possibly conflicting information on the seismological agencies themselves and not the emergency responders.

The following account of the NEIC response to the Tohoku earthquake sequence includes discussion of both internal and publicly distributed products. The account documents the range of products produced by the NEIC and their iterative nature.

Foreshocks

The Tohoku earthquake was preceded by a series of large foreshocks during the prior two days. On March 9, an **M** 7.3 event occurred approximately 40 km east-northeast from the epicenter of the Tohoku earthquake (<http://on.doi.gov/hi1Hr0>), followed by another three earthquakes greater than **M** 6.0 on the same day. As is typical for any major global earthquake, the NEIC released rapid location, magnitude, ShakeMap, and PAGER (Prompt Assessment of Global Earthquakes for Response) products for each event, which were supplemented by USGS *W*-phase moment tensors (Kanamori and Rivera 2008; Hayes, Rivera and Kanamori 2009; Duputel *et al.* 2011) for the **M** 7.3 event and for two of the **M** 6+ earthquakes. A finite fault inversion (Ji *et al.* 2002) for coseismic slip for the **M** 7.3 earthquake showed rupture over an approximately 70 × 50 km patch, with peak slip of ~1.3 m to the north of the hypocenter (<http://on.doi.gov/jKnHd4>).

M_w 9.0 Mainshock

The NEIC response to the mainshock is presented as a timeline constructed with respect to the Origin Time (OT) of the earthquake: Mar 11, 2011, 05:46:23 UTC (Figure 1). The timeline presents a step-by-step view of when hypocentral and magnitude information was derived and released; when subsequent products were compiled and released; and the reasoning behind various decisions made during this real-time response.

OT + 3.8 Minutes: Initial Hypocenter

Origin Time: 05:46:21
Latitude: 38.16
Longitude: 143.25
Depth: 60.0 km

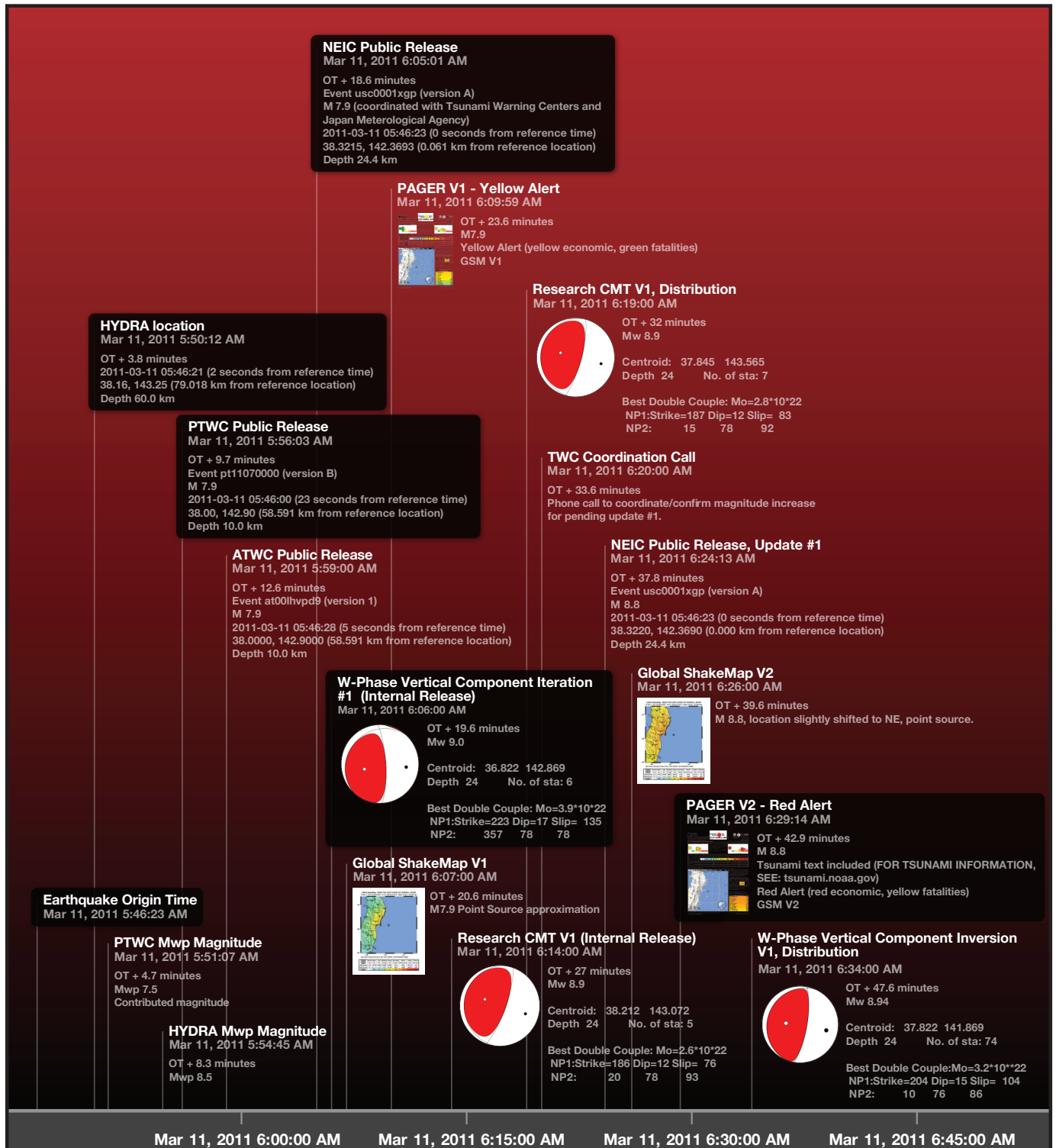
The initial hypocenter for the Tohoku earthquake was obtained in under four minutes by the NEIC real-time processing system, Hydra (Buland *et al.* 2009), using eight *P*-wave observations from stations in Japan, South Korea, and mainland China. This initial location is based on automated picks made from signals filtered to approximately 1 Hz. Using this frequency band, our locations approximate the point of initiation of the rupture process. The earthquake's hypocenter was automatically updated 54 times in the first 47 minutes as real-time data became available from the 83 contributing networks integrated into NEIC operations. The initial location was approximately 80 km away from the (final) reviewed NEIC catalog solution, which is released approximately six–eight weeks after the event. This solution was not released; the location and magnitude of an earthquake is publicly released when the solution becomes stable, which on average occurs within approximately 8–15 minutes of OT for teleseismically derived hypocenters.

OT + 4.7 Minutes: PTWC Observatory Message, M_{wp} 7.5

PTWC released an observatory message, with a magnitude estimate using data from five stations, less than five minutes after OT. Observatory messages are preliminary solutions intended to provide situational awareness to other seismic and tsunami observatories. Because of their preliminary nature, the observatory messages are not displayed on the USGS Web site or distributed through the USGS Earthquake Notification System (ENS). Both PTWC and WCATWC have the mandate to rapidly report earthquakes with the potential to cause tsunamis in their respective regions of responsibility. Their magnitude estimates are often the first public indicators of large events.

OT + 9.7 Minutes: PTWC Tsunami Bulletin Release

Magnitude: 7.9
Origin Time: 05:46:00
Latitude: 38.00
Longitude: 142.90
Depth: 10.0 km



▲ **Figure 1.** Snapshot of the first 50 minutes of the timeline of NEIC event response to the Tohoku earthquake. Each event in the timeline is represented at UTC relative to the earthquake origin time. Major events are highlighted in gray boxes. For the full timeline in QuickTime .MOV format, see the online material.

In just under 10 minutes, PTWC released its first tsunami bulletin. Tsunami bulletins are official NOAA public releases that provide preliminary estimates of an earthquake's magnitude and hypocenter and describe potential near- and far-field tsunami hazard. The earthquake source information contained in tsunami bulletins is automatically transmitted to the USGS. If the USGS has not yet publicly released information related to the event, the source information provided by NOAA is displayed on the USGS Web site and replaced when the USGS releases its own solution.

Following established policy for earthquakes in the Japan region, the initial hypocenter and magnitude used by the NOAA TWCs is coordinated with the Japan Meteorological Agency (JMA). Subsequent bulletin releases often contain updated magnitude and hypocenter estimates that are generally coordinated with the USGS.

OT+18.6 Minutes: NEIC Public Release

Magnitude: 7.9
Origin Time: 05:46:23
Latitude: 38.32
Longitude: 142.37
Depth: 24.4 km

The initial NEIC public release consisted of the hypocenter and origin time from the Hydra system and the **M** 7.9 magnitude coordinated with the NOAA TWCs and JMA. At this time, the NEIC had computed several internal magnitude estimates including $m_b(L_g)$, m_b , m_L , m_B and M_{wp} (Tsuboi *et al.* 1995). All were below **M** 7.8 except M_{wp} , which estimated **M** 8.3. Only M_{wp} was considered for response purposes, because the other available magnitude-types are known to be poor predictors of size for very large events.

If there is compelling evidence to support an early NEIC magnitude over coordinated estimates, then such coordination with the tsunami warning centers is not mandatory. However, at the time of the first public release for the Tohoku earthquake, M_{wp} had decreased from an original estimate of **M** 8.5 (OT + 8.3 minutes) and did not yet appear to have stabilized. Although there were indications the earthquake was larger (including higher M_{wp} estimates from both TWCs), we decided to release the event with **M** 7.9 and update this magnitude when the waveform-based *W*-phase estimates were completed and reviewed. In hindsight, this decision proved to be a significant underestimate, which reflects the tension between providing rapid information and the uncertainties inherent in quickly determining the magnitudes of great earthquakes.

OT + 19.6 Minutes: W-Phase Vertical Component Iteration #1 M_w 9.0

The *W*-phase moment tensor inversion (Kanamori and Rivera 2008) has been running at NEIC in a conditional operation mode since July 2008 (Hayes, Rivera and Kanamori 2009). Results from this system are only used when they have been manually reviewed by a subject matter expert. The inversion

triggers once the initial earthquake location and magnitude is released and runs iteratively, adding data as they become available. Two versions of the inversion are run in parallel: one that uses vertical-component channels only, and one that uses three-component data (Duputel *et al.* 2011).

This initial solution with M_w 9.0 was constrained by few data (six vertical channels) close to the earthquake (20–40°). Experience has shown that early *W*-phase results may vary by as much as ± 0.3 magnitude units; as such, we decided to wait for the inversion to stabilize.

OT + 20.6 Minutes: Global ShakeMap V1

Based on the initial **M** 7.9 release, this first version of Global ShakeMap (Allen and Wald 2009) used ground-motion prediction equations employing a hypocentral-distance approximation (Wald *et al.* 2008). Mapping fault distance to hypocentral distance approximates near-source ground motions when fault dimensions are not yet ascertained (Figure 2).

OT + 23.6 Minutes: PAGER V1

Based on Global ShakeMap V1, the first version of PAGER estimated yellow and green alerts for economic damage and fatalities, respectively (see Figure 2 for an explanation of PAGER alert levels). These alerts were underpredicted because of the initial low magnitude estimate. This alert was distributed to a list of critical users (*e.g.*, first responders, government agencies, aid agencies, and critical facilities), and to the NEIC event pages online (Figure 2).

OT + 32 Minutes: Research CMT Internal Distribution M_w 8.9

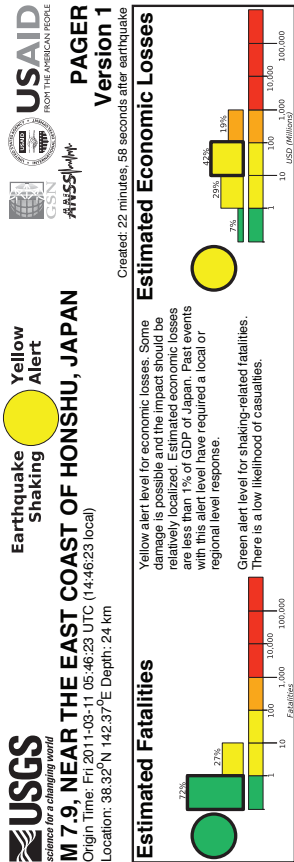
The centroid moment tensor inversion algorithm at the USGS is based on the inversion approach of Jascha Polet (California State Polytechnic University, Pomona), who runs an internally distributed routine at the NEIC that, like *W* phase, triggers off the initial NEIC release (Polet and Thio forthcoming). The distributed solution of this inversion, after just 32 minutes and using seven channels of data, gave M_w 8.9, providing key confirmation of the initial *W*-phase **M** 9.0 moment tensor, indicating that a true mega-earthquake had just occurred.

OT + 38 Minutes: NEIC/PTWC Coordinated Magnitude Update

Magnitude: 8.8
Origin Time: 05:46:23
Latitude: 38.32
Longitude: 142.37
Depth: 24.4 km

The first update of the NEIC public release used the location and origin time from the Hydra system, while magnitude was coordinated with that of the TWCs. Communication between the TWCs and NEIC confirmed the research CMT results,

(A)



Estimated Population Exposed to Earthquake Shaking

ESTIMATED POPULATION EXPOSURE (k = x1000)	719k	0	0	0					
ESTIMATED MODIFIED MERCALLI INTENSITY	I	II-III	IV	V	VI	VII	VIII	IX	X+
PERCEIVED SHAKING	Not felt	Weak	Light	Moderate	Strong	Very Strong	Severe	Violent	Extreme
POTENTIAL DAMAGE	none	none	none	Light	Moderate	Moderate/Heavy	Heavy	V. Heavy	V. Heavy
Resistant Structures	none	none	none	Light	Moderate	Moderate/Heavy	Heavy	V. Heavy	V. Heavy
Vulnerable Structures	none	none	none	Light	Moderate	Moderate/Heavy	Heavy	V. Heavy	V. Heavy

Population Exposure
Estimated exposure only includes population within the map area.

Population Exposure
population per ~1 sq. km from Landsat



Structures:
Overall, the population in this region resides in structures that are resistant to earthquake shaking. The predominant vulnerable building types are ductile reinforced concrete frame and heavy wood frame construction.

Historical Earthquakes (with MMI levels):

Date (UTC)	Dist. (km)	Mag.	Max Shaking (MMI#)	Deaths
1988-06-14	363	5.7	VII(428k)	0
1994-12-28	263	7.7	VII(132k)	3
1983-05-26	369	7.7	VII(174k)	104

Recent earthquakes in this area have caused secondary hazards such as tsunamis, landslides, and fires that might have contributed to losses.

Selected City Exposure

MMI City	Population
VII Ishinomaki	117k
VII Yamoto	32k
VII Shiogama	60k
VII Kogota	20k
VII Rifu	35k
VII Ofunato	35k
VI Sendai	1,038k
VI Yamagata	255k
VI Morioka	295k
IV Utsunomiya	294k
IV Utsunomiya	450k

bold cities appear on map (k = x1000)

PAGER content is automatically generated, and only considers losses due to structural damage. Limitations of input data, shaking estimates, and loss models may add uncertainty.
<http://earthquake.usgs.gov/pager>

Event ID: usc0001xgp

(B)

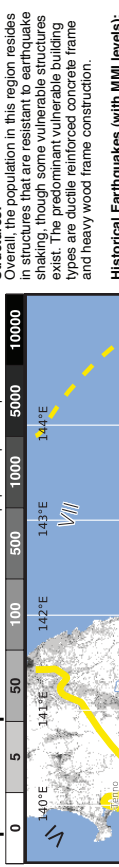


Estimated Population Exposed to Earthquake Shaking

ESTIMATED POPULATION EXPOSURE (k = x1000)	7,081k	1,876k	0	0					
ESTIMATED MODIFIED MERCALLI INTENSITY	I	II-III	IV	V	VI	VII	VIII	IX	X+
PERCEIVED SHAKING	Not felt	Weak	Light	Moderate	Strong	Very Strong	Severe	Violent	Extreme
POTENTIAL DAMAGE	none	none	none	V. Light	Light	Moderate	Moderate/Heavy	Heavy	V. Heavy
Resistant Structures	none	none	none	V. Light	Light	Moderate	Moderate/Heavy	Heavy	V. Heavy
Vulnerable Structures	none	none	none	V. Light	Light	Moderate	Moderate/Heavy	Heavy	V. Heavy

Population Exposure
Estimated exposure only includes population within the map area.

Population Exposure
population per ~1 sq. km from Landsat



Structures:
Overall, the population in this region resides in structures that are resistant to earthquake shaking, though some vulnerable structures exist. The predominant vulnerable building types are ductile reinforced concrete frame and heavy wood frame construction.

Historical Earthquakes (with MMI levels):

Date (UTC)	Dist. (km)	Mag.	Max Shaking (MMI#)	Deaths
1988-06-14	363	5.7	VII(428k)	0
1994-12-28	263	7.7	VII(132k)	3
1983-05-26	369	7.7	VII(174k)	104

Recent earthquakes in this area have caused secondary hazards such as tsunamis, landslides, and fires that might have contributed to losses.

Selected City Exposure

MMI City	Population
VIII Ishinomaki	117k
VIII Yamoto	32k
VIII Shiogama	60k
VIII Kogota	20k
VIII Rifu	35k
VIII Furukawa	76k
VII Sendai	1,038k
VII Yamagata	255k
VII Morioka	295k
VII Fukushima	294k
VI Utsunomiya	450k

bold cities appear on map (k = x1000)

PAGER content is automatically generated, and only considers losses due to structural damage. Limitations of input data, shaking estimates, and loss models may add uncertainty.
<http://earthquake.usgs.gov/pager>

Event ID: usc0001xgp

▲ **Figure 2.** Versions 1 (A), 2(B), 5(C), and 12 (D; current at time of publication) of the USGS PAGER report for the Tohoku earthquake. Each panel shows the population (from LandScan 2008, Oakridge National Laboratory) exposed to each level of shaking estimated by the USGS ShakeMap. The gray-scale shading in the map display represents population density, also listed by shaking intensity in the table above. The uppermost display summarizes the alert level of the earthquake, based on models of economic losses and fatalities. The higher of the two alert levels gives the summary alert level, at the top of each panel. The table in the lower-right corner of each summary lists the population of nearby major cities and their exposure levels. Above this, a list of nearby historically damaging earthquakes is given, with a summary of regional structural vulnerability.

(D)



Earthquake Shaking Red Alert

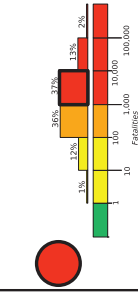
M 9.0, NEAR THE EAST COAST OF HONSHU, JAPAN

Origin Time: Fri 2011-03-11 05:46:23 UTC (14:46:23 local)

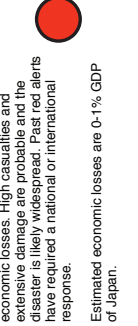
Location: 38.32°N 142.37°E Depth: 32 km

FOR TSUNAMI INFORMATION, SEE: tsunami.noaa.gov

Estimated Fatalities



Estimated Economic Losses



PAGER Version 12

Created: 2 weeks, 1 day after earthquake

Estimated Economic Losses

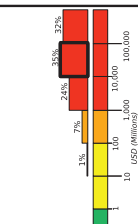


Table with 4 columns: ESTIMATED POPULATION EXPOSURE, ESTIMATED MODIFIED MERCALLI INTENSITY, PERCEIVED SHAKING, POTENTIAL DAMAGE. Rows include intensity levels I through IX+ and corresponding shaking descriptions like 'Not felt', 'Weak', 'Light', etc.

Overall, the population in this region resides in structures that are resistant to earthquake shaking, though some vulnerable structures exist.



Historical Earthquakes (with MMI levels): Table with 4 columns: Date (UTC), Dist. (km), Mag., Max Shaking (MMI), Deaths. Lists earthquakes from 1986 to 1994.

Selected City Exposure table with 2 columns: MMI City, Population. Lists cities like Furukawa, Iwanuma, Hitachi, etc., with their corresponding MMI and population.

PAGER content is automatically generated, and only considers losses due to structural damage. Limitations of input data, shaking estimates, and loss models may add uncertainty.

http://earthquake.usgs.gov/pager

Event ID: usc0001xgp

(C)



Earthquake Shaking Red Alert

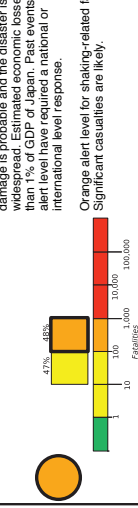
M 8.9, NEAR THE EAST COAST OF HONSHU, JAPAN

Origin Time: Fri 2011-03-11 05:46:23 UTC (14:46:23 local)

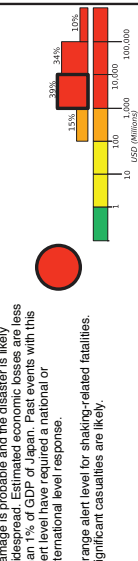
Location: 38.32°N 142.37°E Depth: 24 km

FOR TSUNAMI INFORMATION, SEE: tsunami.noaa.gov

Estimated Fatalities



Estimated Economic Losses



PAGER Version 5

Created: 2 hours, 44 minutes after earthquake

Estimated Economic Losses

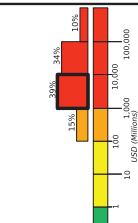


Table with 4 columns: ESTIMATED POPULATION EXPOSURE, ESTIMATED MODIFIED MERCALLI INTENSITY, PERCEIVED SHAKING, POTENTIAL DAMAGE. Rows include intensity levels I through IX+ and corresponding shaking descriptions like 'Not felt', 'Weak', 'Light', etc.

Overall, the population in this region resides in structures that are resistant to earthquake shaking, though some vulnerable structures exist.



Historical Earthquakes (with MMI levels): Table with 4 columns: Date (UTC), Dist. (km), Mag., Max Shaking (MMI), Deaths. Lists earthquakes from 1986 to 1994.

Selected City Exposure table with 2 columns: MMI City, Population. Lists cities like Omiyawa, Oarai, Hasaki, etc., with their corresponding MMI and population.

PAGER content is automatically generated, and only considers losses due to structural damage. Limitations of input data, shaking estimates, and loss models may add uncertainty.

http://earthquake.usgs.gov/pager

Event ID: usc0001xgp

▲ Figure 2 (continued). Versions 1 (A), 2(B), 5(C), and 12 (D); current at time of publication) of the USGS PAGER report for the Tohoku earthquake. Each panel shows the population (from LandScan 2008, Oakridge National Laboratory) exposed to each level of shaking estimated by the USGS ShakeMap. The gray-scale shading in the map display represents population density, also listed by shaking intensity in the table above. The uppermost display summarizes the alert level of the earthquake, based on models of economic losses and fatalities. The higher of the two alert levels gives the summary alert level, at the top of each panel. The table in the lower-right corner of each summary lists the population of nearby major cities and their exposure levels. Above this, a list of nearby historically damaging earthquakes is given, with a summary of regional structural vulnerability.

WATWC M_{wp} , and the W -phase results calculated by NEIC and PTWC, all between M 8.8 and M 9.0. While manual review continued to finalize NEIC's three-component W -phase results, it was clear the initial magnitude needed a rapid update.

OT + 40 Minutes: Global ShakeMap V2

OT + 43 Minutes: PAGER V2

Based on Global ShakeMap V2 (as V1, with the updated M 8.8 magnitude), this second version of PAGER estimated red and yellow alerts for shaking-related economic damage and fatalities, respectively. This alert was distributed to a list of critical users (e.g., first responders, government agencies, aid agencies, and critical facilities) after a 10-minute verification-based delay, and to the NEIC event pages online. At this stage, text referring the reader to the NOAA Web site (<http://www.tsunami.noaa.gov>) was also included on the *onepager* (summary) alert.

OT + 48 Minutes: W-Phase Vertical Component Solution

Distribution

M_w 8.9

The final automatic solution of the vertical-component W -phase inversion running at the NEIC, using 74 channels of data (15–90°), suggested M_w 8.94. This solution was distributed internally.

OT + 62 Minutes: W-Phase Three Component Solution

Distribution

M_w 8.9

The final automatic solution of the three-component W -phase inversion running at the NEIC, using 89 channels of data, suggested M_w 8.90, and was distributed broadly to subscribed users and to the NEIC event pages online.

OT + 65 Minutes: Magnitude Update, NEIC Public Release

Magnitude: 8.9

Origin Time: 05:46:23

Latitude: 38.32

Longitude: 142.37

Depth: 24.4 km

The second update of the NEIC public release was based on the same location and origin time, with magnitude updated based on the NEIC three-component W -phase inversion solution.

OT + 1 Hour, 09 Minutes: Global ShakeMap V3

OT + 1 Hour, 16 Minutes: PAGER V3

This magnitude update again triggered updates to ShakeMap and PAGER; the revised magnitude increased the PAGER shaking-induced fatalities alert level to orange. PAGER alert levels remained stable (red for economic losses, orange for fatalities) from this stage onward, until data released several

days after the event slightly increased estimated fatalities and changed the fatality-based alert level to red.

OT + 1 Hour, 35 Minutes: Tectonic Summary Posted

As with all major earthquakes, the NEIC produced a tectonic summary for the Tohoku event, describing the broad tectonics of the source region, the plates involved in the earthquake and their relative motion rates, the likely source fault(s) hosting the earthquake rupture, and recent nearby historic earthquake activity.

Subsequent iterations of this tectonic summary, posted in the days following the event, provided more detail regarding the historic earthquake activity of the region, particularly in relation to large and tsunamigenic earthquakes. These summaries were also provided in a Spanish version, which was available several hours after the initial release.

OT + 1 Hour, 45 Minutes–2 Hours, 35 Minutes: Finite Fault Inversion, Iterations #1 and #2

The initial finite fault inversion used a fault geometry guided by the results of the automated three-component W -phase inversion solution, which had a strike misaligned with the geometry of the Japan Trench (230° vs. approximately 195°, respectively); thus, the results of this initial solution were misrepresentative of the rupture process. The fault plane strike was realigned based on information from local slab geometry (USGS Slab1.0 model, <http://on.doi.gov/d9ARbS>; Hayes, Wald and Keranen 2009), and the data re-inverted. The subsequent solution (V2, OT + 2 hours, 35 minutes) identified a bilateral rupture, approximately 300 km in length, with two major asperities to the north and south, respectively, centered on the ~60 second isochron.

OT + 2 Hours, 42 Minutes: Global ShakeMap V4, Finiteness

Approximate finite fault dimensions were added to the ShakeMap at this time based on a combination of finite fault inversion results and the overall aftershock distribution, both of which suggested a slightly bilateral rupture, dominantly southward, approximately 300 km in length. ShakeMap also included results from several hundred *Did You Feel It?* (DYFI?) macroseismic surveys. Though the finite fault dimensions were later refined (as noted below), the initial estimates proved effective for the purposes of the ground-motion prediction equations used. The estimated shaking-based losses from the PAGER system with this approximate model proved consistent with the known shaking-related losses at the time of this writing.

OT + 6 Hours, 04 Minutes: W-Phase Three Component Solution, Manual Update and Redistribution

M_w 9.0

After distribution and publication of the initial automated solution, and as more data became available through the NEIC

waveform buffer, the W -phase inversion was refined, paying particular attention to the quality of inverted data. After several further iterations, this inversion with 234 data channels suggested a moment magnitude of M_w 8.99. The best double couple of this solution was also well aligned with local slab geometry. This CMT was distributed internally at OT + 5 hours, 17 minutes and published to the NEIC event pages 47 minutes later. Given the small magnitude change (0.1 units) and the likelihood of further updates and refinements to W phase over the following hours/days, the NEIC kept its official magnitude at **M** 8.9 pending the expected review.

OT + 6 Hours, 55 Minutes: Finite Fault Inversion, Iteration #3c
 M_w 9.0

Two features prompted a re-inversion of the V2 solution; first, the relatively slow start to the earthquake (indicated by low moment rate over the first ~50 s of rupture) and the parameterization of rupture velocity (initially constrained to a range from 1.9 to 3.3 km/s) forced rupture away from the hypocenter in the V2 solution. The rupture velocity range was thus adjusted to allow rupture close to the hypocenter, if preferred by the inverted data. Second, maximum slips in the V2 solution were constrained to 15 m; this was increased to allow for larger slips in what appeared to be a compact rupture (limited to ~150 s of high moment rate, within 300 km of the hypocenter in these initial inversions).

In version 3, fault geometry was correctly aligned, rupture velocity bounds were broad (0.5–3.5 km/s), and peak slips were less constrained. After careful data realignment, and further relaxation of moment minimization restrictions (allowing moment to be constrained by the inverted data—principally surface waves—rather than the input CMT solution), version 3C indicated bilateral rupture, approximately 300 km in length along strike, up-dip of the hypocenter toward the Japan Trench, with peak slips of approximately 18 m. This solution (OT + 6 hours, 55 minutes) was distributed internally and published on the NEIC event pages approximately three hours later (Figure 3).

OT + 1–24 Hours: Press Response

Throughout the day following the Tohoku earthquake, the NEIC received a significant media response to the event, as did USGS offices across the country in Menlo Park, CA; Pasadena, CA; Reston, VA; Anchorage, AK; and Seattle, WA.

A team of NEIC analysts, communications staff, and researchers responded to incoming media enquiries nearly continuously starting minutes after the earthquake through the following day. Both local and national news agencies came to the NEIC offices to conduct a succession of live media reports about various aspects of the earthquake and its devastating tsunami, including a live evening news broadcast from our media center. A near continuous stream of interviews were conducted in the 24 hours following the earthquake; several tens more were conducted over the subsequent week.

OT + 7 Hours, 19 Minutes: Global Centroid Moment Tensor (gCMT) Solution, V1 Distribution
 M_w 9.1

Soon after the release of the updated W -phase inversion solution (M_w 9.0) and the initial fast finite fault model, the gCMT group (<http://www.globalcmt.org>) released its initial estimate of the moment tensor of the Tohoku earthquake, indicating a moment magnitude of M_w 9.12. The dip of the shallow plane of the best-fitting double couple to this solution (strike = 201°, dip = 09°, rake = 85°) was much shallower than that of the W -phase solution (strike = 193°, dip = 14°, rake = 81°), indicating that the difference in moment between the two solutions (6.0×10^{29} dyne-cm gCMT vs. 3.9×10^{29} dyne-cm W phase) may be related to the well-known moment-dip tradeoff for shallow earthquakes first noted by Kanamori and Given (1981). Nevertheless, this discrepancy was an indication that further detailed analyses were warranted.

Approximately three days later, gCMT updated its inversion results to a solution with moment magnitude M_w 9.08, with a similar mechanism (strike = 203°, dip = 10°, rake = 88°).

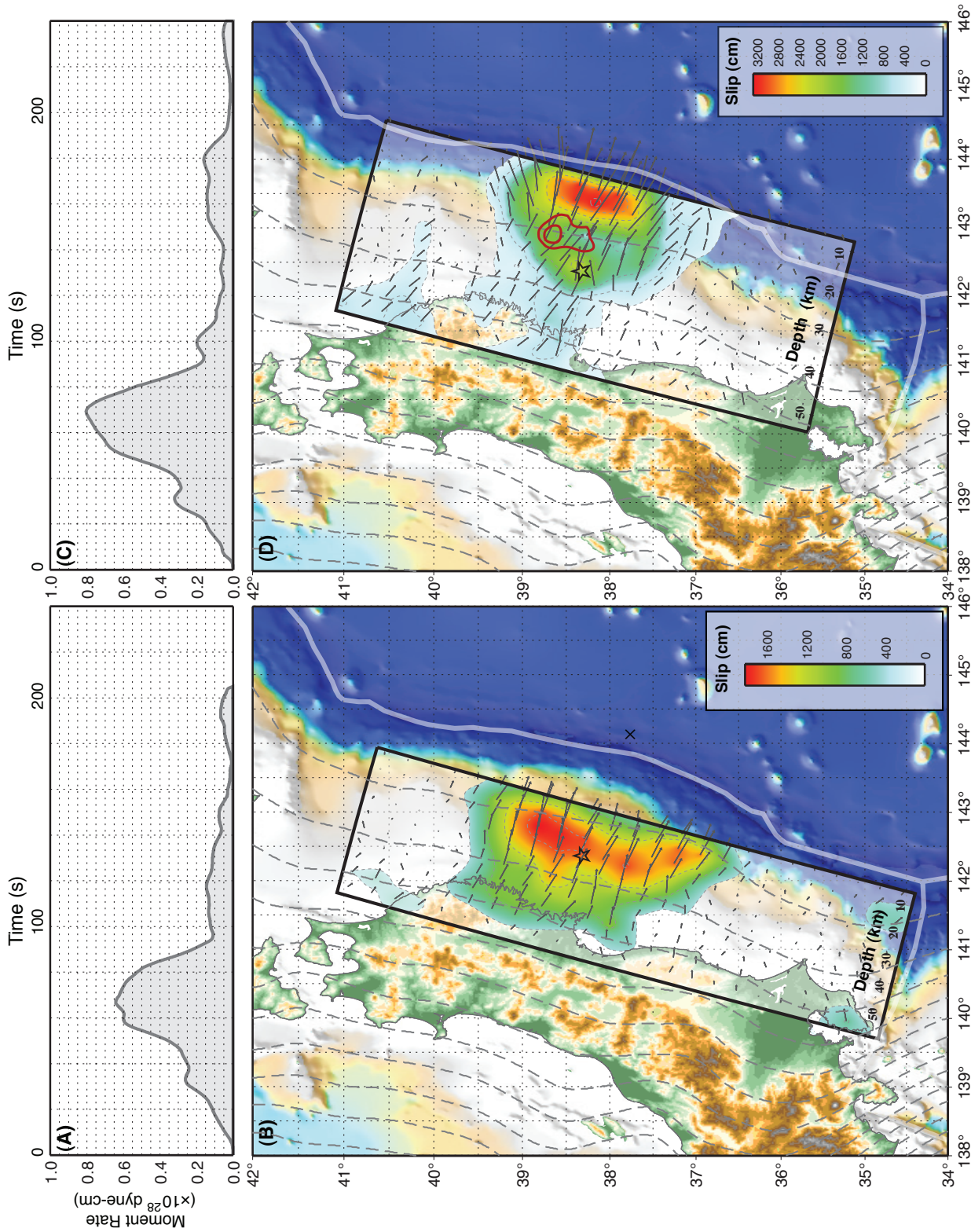
OT + 8 Hours: Summary Poster Distribution

The initial version of the USGS summary poster, describing tectonic setting, local seismic hazard, regional seismicity, and rapid results from ShakeMap and PAGER, was available on the NEIC event pages approximately eight hours after the event.

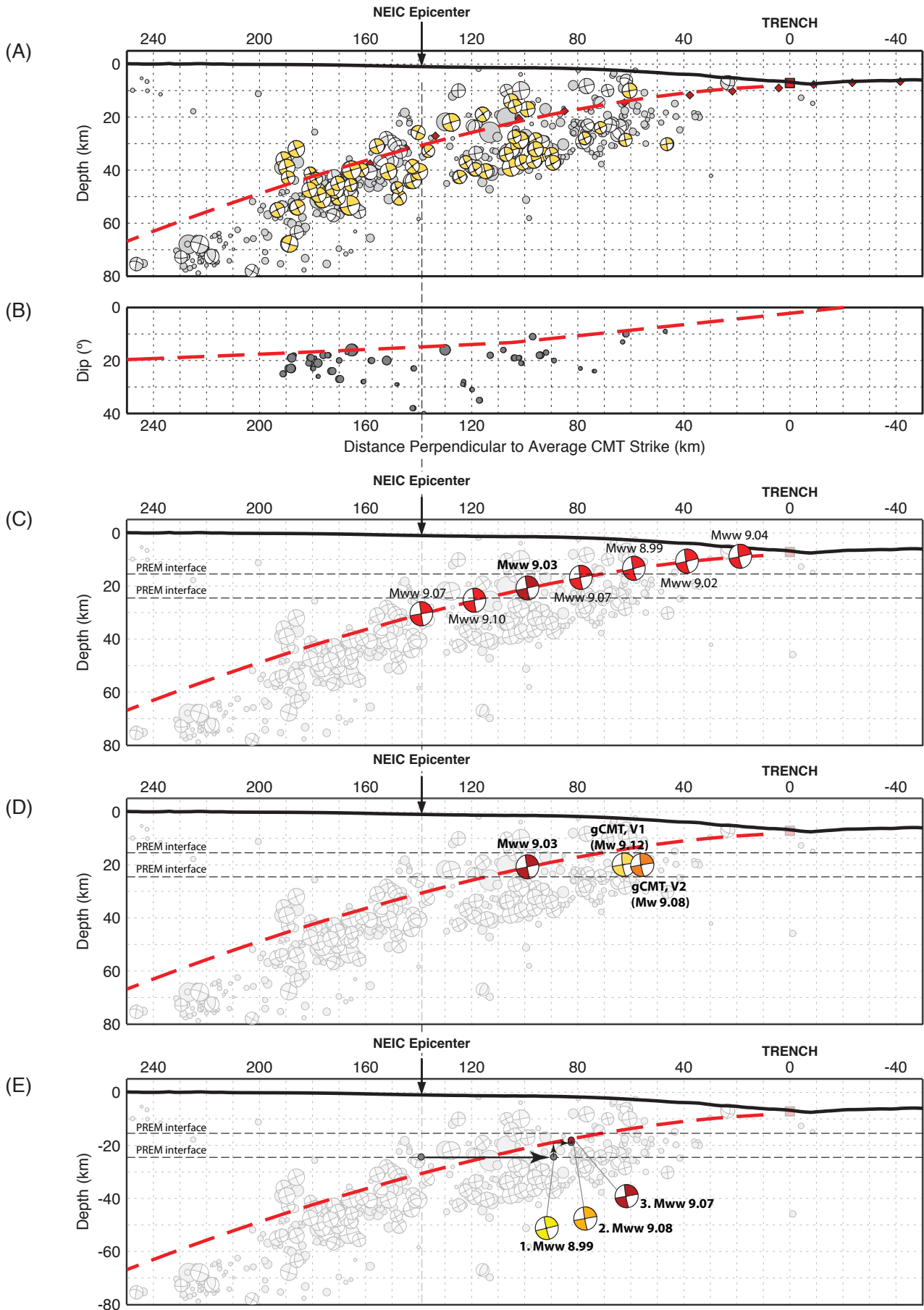
OT + 2 Days: W-Phase Dip Sensitivity Analyses
 M_w 9.0

Over the next days, magnitude estimates were further refined. This included follow-up discussions with Louis Rivera at the Institut de Physique du Globe de Strasbourg (University of Strasbourg, France), Jascha Polet at Cal Poly Pomona, and Meredith Nettles at the Lamont-Doherty Earth Observatory. Magnitude estimates obtained by our studies and by these researchers using different data and techniques were close, generally within 0.1 magnitude units.

The final USGS magnitude estimate of **M** 9.0 is based on an in-depth review of the USGS W -phase results, and matches the final (current) official estimate of the JMA. The USGS **M** 9.0 was obtained after testing the sensitivity of the W -phase inversion to centroid location, depth, and (indirectly) to inverted dip, by carrying out a series of fixed-centroid inversions at intervals along the modeled surface of the slab (from the USGS Slab1.0 model; Figure 4) using the filtered data set from the published, updated W -phase inversion solution. Both the ability of the inversion to recover the geometry of the slab interface at the fixed location, and the root mean square misfit of the synthetics to the data, were used to infer the best-fitting solution. Results showed some sensitivity to interfaces in the PREM velocity model (Dziewonski and Anderson 1981) used in the inversion procedure, but the preferred solution indicated a depth of 21 km, a dip of 12°, and a moment magnitude of M_w 9.03 (Figure 4).



▲ **Figure 3.** Maps of the initial (A, B) and updated (C, D) USGS NEIC finite fault slip distributions of the Tohoku earthquake. Panels (A) and (C) show source time functions of each solution. In each map panel (B) and (D), the inverted slip distribution is shown within the assumed rectangular fault geometry, colored by slip magnitude, and contoured every 4 m. Regions with slip below 4 m are partially transparent. The slip vector of each subfault is represented with a gray arrow, also scaled by slip magnitude. On panel (D), red contours represent the 0.5 and 1.0 m slip distributions of the 9 March 2011 M_w 7.3 foreshock



Considering updated W -phase results and our in-depth dip sensitivity analyses, the USGS/NEIC decided to update its magnitude classification of the Tokoku earthquake with a coincident press release about three and a half days after the event (<http://on.doi.gov/gcBgWv>). JMA also updated its magnitude estimate of the event to **M** 9.0 after independent analyses.

DISCUSSION

Fortunately, great earthquakes such as the Tohoku event are infrequent. The timeline presented above allows for critical evaluation of NEIC response to a rare, outsized earthquake. The NEIC's core response—the rapid determination of earthquake location and size and the immediate dissemination of this information—was sound. The NEIC also delivered (and subsequently updated) further products such as ShakeMap and PAGER quickly and accurately. In the sections below we discuss the evolution of earthquake magnitude, ShakeMap, PAGER, and finite fault models, and provide context for decisions to issue updates. When compared to the similar 2004 **M** 9.1 Sumatra-Andaman earthquake, response to the Tohoku event was uniformly faster and (in retrospect) more accurate. Room for improvement remains on several fronts, particularly in coordination of initial magnitude and its updates, and the use of a priori fault geometries for rapid finite fault models.

Evolution of Earthquake Magnitude

Within 65 minutes of the origin time of the Tohoku earthquake, the magnitude estimated by the NEIC was updated twice, from the initial coordinated release at **M** 7.9 (OT+18.6 minutes) to **M** 8.9 (OT + 65 minutes). Within 20 minutes, W -phase algorithms had obtained preliminary estimates of the great size (M_w 9.0 from W -phase vertical component iteration #1, OT + 19.6 minutes) and thus the potentially devastating impacts of the event. Three days later, the magnitude estimate was updated a final time to M_w 9.0, reflecting more detailed analyses of the event. This final change, while important for accurate descriptions of the event and for detailed analyses that will follow, would not have significantly affected the real-time estimates of the impact of the earthquake as reflected by the stability in the USGS ShakeMap and PAGER products at **M** 8.9 versus **M** 9.0. Future work will focus on reconciling uncertainties in initial

magnitudes (particularly using W -phase and rapid CMT estimates for such large earthquakes) with the NEIC mandate to release limited, authoritative magnitude measurements.

It is illuminating to compare NEIC responses to the 2011 Tohoku and the great M_w 9.1 26 December 2004 Sumatra-Andaman Islands earthquakes. In the latter case, the initial automatic NEIC solution (not a public release) came after 17 minutes, with an m_b of 6.2. After 10 more minutes, an automatic CMT solution gave the first internal indication of the large size of the earthquake, with a moment magnitude of M_w 8.2. One hour and 23 minutes after OT, parameters were publicly released using an M_s magnitude of 8.5. The magnitude was later updated to M_w 8.9 after six hours and 13 minutes, based on the preliminary global CMT (at that time, Harvard CMT) solution. Importantly, at that time NEIC was dependent on others to provide an authoritative measure of earthquake size.

NEIC's response to the 2011 Tohoku earthquake was uniformly faster than the response to the Sumatra-Andaman Islands event in 2004. The **M** 7.9 initial public magnitude release for the Tohoku event (OT + 18.6 minutes), while considerably lower than the final magnitude, occurred nearly one hour faster than the first magnitude release in 2004 (OT + 77 minutes). More importantly, in 2011 NEIC publicly updated the magnitude in 38 minutes to **M** 8.8 and to **M** 8.9 in 65 minutes, after internal algorithms rapidly indicated the much larger size of the event.

If the 2011 and 2004 timelines are overlain and compared, a magnitude update in 2011 to within 0.1 units of the final magnitude was made before any official information regarding the great size of the 2004 Sumatran earthquake had been publicly distributed. In other words, in 2011 the world was aware of the great size of the Tohoku event in minutes to hours, while in 2004 it took hours to days for information to be disseminated.

Much of this dramatic improvement has been brought about by operational and institutional changes that have occurred since 2004 as either direct or indirect consequences of the Sumatran earthquake, through investments made in the GSN, the NEIC, and in research and development on rapid characterization of great earthquake sources. Most significantly, the NEIC has changed to a 24/7 operational facility, rather than utilizing analysts and researchers on an on-call basis outside of regular office hours. We have benefited from the expertise of academic partners through external-grant programs and from in-kind support that has allowed us to install, test, and operate rapid and accurate source-based analyses than

▲ **Figure 4.** Subduction geometry from the USGS Slab1.0 model, and W -phase resolution tests for earthquake centroid and dip. Panel (A) shows a cross-section of the subduction zone through the epicenter of the mainshock (vertical dashed line), overlain with a 2D profile through Slab1.0. Yellow CMTs are gCMT solutions used to constrain the slab geometry; gray circles and mechanisms represent background seismicity. Red diamonds represent data from local active seismic surveys, also used to constrain geometry. See <http://earthquake.usgs.gov/research/data/slab/> for more details. Panel (B) shows the dip of the Slab1.0 interface. Gray circles show the dips of yellow mechanisms from panel (A). In panel (C), we show W -phase CMT inversions at fixed centroid locations along the slab interface, to test the sensitivity of the inversion to location and its ability to resolve slab interface dip. The favored solution is shown in maroon; others in red. In panel (D), we show this solution with respect to the initial and updated gCMT solutions. Finally, in panel (E) we show an iterative W -phase inversion solution, in which centroid location is permitted to change horizontally but not vertically. After each iteration the centroid location is shifted to the Slab1.0 interface, and the data are re-inverted from the new location. This process is continued until the centroid location no longer shifts from the starting location, resulting in mechanism #3, in maroon.

were not routinely available six years ago, such that earthquake magnitude (and other source-based observations like rupture duration and finiteness) can be described in a more timely and precise manner than was previously possible. Finally, through both new hires and direct event-based experience, we have built a team of analysts and researchers and have established procedures that in turn facilitate more fluent, accurate, and coordinated earthquake response efforts.

In contrast, when faced with an M 9.1 event in 2004, the NEIC lacked a comprehensive set of tools to rapidly provide a scientific framework and estimate the societal impact of the event. Today, the challenge has evolved to addressing how we refine these tools to work better in tandem, and how to better streamline our external coordination efforts.

Evolution of ShakeMap and PAGER

ShakeMap and PAGER are USGS products that translate earthquake information into maps of expected ground shaking and estimates of fatalities and economic losses. Both rely on rapid source evaluation and prompt dissemination of updates for their usefulness. Rather than a detailed evaluation of ShakeMap and PAGER for this event, we focus here on the connection between these products and magnitude, fault geometry, and slip updates.

Preliminary estimates of ShakeMap shaking distributions and PAGER population exposure (Figure 2) were low relative to final estimates because they relied on the low (M 7.9) initial earthquake magnitude. Both ShakeMap shaking distributions and PAGER exposure estimates and alert levels rapidly increased toward their final estimates as magnitude estimates were updated (OT + 1 hour, 09 minutes: Global ShakeMap V3; OT + 1 hour, 16 minutes: PAGER V3).

Large earthquakes require approximate fault geometries in order to generate accurate updates to initial ShakeMap and PAGER analyses. ShakeMap was updated to include data from regional *DYFI?* questionnaires and fault-finiteness information—that is, the length and width of the rupture area—two hours and 40 minutes after OT (ShakeMap version 4). The initial estimates of fault dimensions (based on aftershock distributions) were revised on 2011-03-14 when the National Research Institute for Earth Science and Disaster Prevention (NIED) in Japan released estimates of slip distribution from the inversion of strong-motion data (ShakeMap version 5). A subset of strong-motion data recorded by K-Net became available the following day, on 2011-03-15, and was incorporated into ShakeMap at that time (ShakeMap version 6). Similarly, a subset of KiK-Net strong-motion data was released on 2011-03-19, leading to ShakeMap version 8. Full K-Net and KiK-Net data sets were released on 2011-03-23 and 2011-03-26, respectively, and led to the final ShakeMap updates, ShakeMap versions 10–12. None of the subsequent versions diverged substantially from ShakeMap version 4, released less than three hours after the event.

PAGER is updated each time a new ShakeMap becomes available. Alert levels changed to orange for fatalities 75 minutes after the earthquake, having become a red alert (based

on economic loss estimates) after the first magnitude update at OT + 43 minutes. PAGER remained at these levels until ShakeMap version 10, when the full distribution of K-Net and KiK-Net data became available. Some of these data showed higher recorded ground motions than previously observed or estimated, leading to changes in ShakeMap and a corresponding increase in the PAGER fatality alert level to red.

Evolution of Finite Fault Models

Finite fault models provide a time history of slip along an earthquake rupture. Most important for rapid hazard estimation, the culmination of these models is a map of static slip on the fault plane. Estimates of rupture length and maximum slip derived from finite fault models are important constraints on maps of expected ground shaking and estimates of population exposure.

Early estimates (V1 and V2) of fast finite fault slip distributions derived from teleseismic data suffered from misaligned fault geometry with respect to slab structure and from difficulties in rupture velocity and peak slip parameterization. These issues were corrected by using a priori geometry information from Slab1.0 and by allowing a broad range of rupture velocities and slip in the inversion procedure, resulting in version 3 of the model, which provided the first accurate estimate of the distribution of slip on the Japan Trench subduction zone. This model was available and distributed internally within seven hours of OT. While this model has since been updated (Figure 3; also see <http://on.doi.gov/h32IYb>) to better account for fault geometry, data distribution and quality, and other detailed aspects of the modeling procedure, the general along-strike and up-dip distribution of slip estimated by this first model is very similar to those shown in a variety of models released since that time. More details of these models and exploration of their sensitivities can be found in Hayes (forthcoming). Figure 3 also shows the relation of slip during the 03/09 M_w 7.3 foreshock to that of the mainshock, indicating that the Tohoku earthquake may have re-ruptured the same patch as the foreshock, albeit with low slip with respect to averages.

Uncertainty in the nodal planes of early moment tensor estimates speaks to the usefulness of using a priori information, such as from models like Slab1.0, to constrain initial fault geometries. The use of Slab1.0 for future major subduction zone earthquakes could decrease the time to first slip distribution estimates by as much as two-thirds, given a case similar to the Tohoku earthquake.

SUMMARY

This article presents a timeline of NEIC response to a major global earthquake for the first time in a formal journal publication. We outline the key observations of the earthquake made by the NEIC and its partner agencies, discuss how these analyses evolved, and outline when and how this information was released to the public and to other internal and external parties. Our goal in the presentation of this material is to provide a detailed explanation of the issues faced in the response to a

rare, giant earthquake. We envisage that the timeline format of this presentation can highlight technical and procedural successes and shortcomings, which may in turn help prompt research by our academic partners and further improvements to our future response efforts. We have shown how NEIC response efforts have significantly improved over the past six years since the great 2004 Sumatra-Andaman earthquake. We are optimistic that the research spawned from this disaster, and the unparalleled dense and diverse data sets that have been recorded, can lead to similar—and necessary—improvements in the future. ☒

ACKNOWLEDGMENTS

This manuscript represents a summary of work performed by a team of analysts and researchers at the NEIC, broader USGS, and the NOAA Tsunami Warning Centers; we thank everyone involved in the response to this earthquake for their extraordinary efforts. Luis Rivera and Ryan Gold provided thorough and thoughtful reviews of this manuscript—we thank them, and an anonymous reviewer, for their comments. Data used for real-time analyses discussed here are predominantly from the IRIS/USGS Global Seismic Network. Figures and movies accompanying this manuscript were made with BeeDocs Timeline 3D software (<http://www.beedocs.com/>) and the Generic Mapping Tools software (Wessel and Smith 1998).

REFERENCES

- Allen, T. I., and D. J. Wald (2009). *Evaluation of Ground-Motion Modeling Techniques for Use in Global ShakeMap: A Critique of Instrumental Ground-Motion Prediction Equations, Peak Ground Motion to Macroseismic Intensity Conversions, and Macroseismic Intensity Predictions in Different Tectonic Settings*. USGS Open-File Report 2009-1047, 114 pp.
- Buland, R. P., M. Guy, D. Kragness, J. Patton, B. Erickson, M. Morrison, C. Bryon, D. Ketchum, and H. Benz (2009). Comprehensive seismic monitoring for emergency response and hazard assessment: Recent developments at the USGS National Earthquake Information Center. *Eos, Transactions, American Geophysical Union* **90** (52), Fall Meeting Supplement, Abstract S11B-1696.
- Butler, R., T. Lay, K. Creager, P. Earl, K. Fischer, J. Gaherty, and G. Laske *et al.* (2004). The Global Seismographic Network surpasses its design goal. *Eos, Transactions, American Geophysical Union* **85** (23); doi:10.1029/2004EO230001.
- Duputel, Z., L. Rivera, H. Kanamori, and G. Hayes (2011). W -phase fast source inversion for moderate to large earthquakes (M_w 6.5, 1990–2010). Submitted to *Geophysical Journal International*.
- Dziewonski, A. M., and D. L. Anderson (1981). Preliminary Reference Earth Model (PREM). *Physics of the Earth and Planetary Interiors* **25**, 297–356.
- Hayes, G. P. (forthcoming). Rapid source characterization of the 03-11-2011 M_w 9.0 Tohoku Earthquake. *Earth, Planets and Space*.
- Hayes, G. P., L. Rivera, and H. Kanamori (2009). Source inversion of the W phase: Real-time implementation and extension to low magnitudes. *Seismological Research Letters* **80**, 817–822; doi: 810.1785/gssrl.1780.1785.1817.
- Hayes, G. P., D. J. Wald, and K. Keranen (2009). Advancing techniques to constrain the geometry of the seismic rupture plane on subduction interfaces a priori: Higher-order functional fits. *Geochemistry, Geophysics, Geosystems* **10**; doi:10.1029/2009GC002633.
- Ji., C., D. J. Wald, and D. V. Helmberger (2002). Source description of the 1999 Hector Mine, California, earthquake, part I: Wavelet domain inversion theory and resolution analysis. *Bulletin of the Seismological Society of America* **92**, 1,192–1,207.
- Kanamori, H., and J. W. Given (1981). Use of long-period surface waves for rapid determination of earthquake source parameters. *Physics of the Earth and Planetary Interiors* **27**, 8–31.
- Kanamori, H., and L. Rivera (2008). Source inversion of W phase: Speeding up seismic tsunami warning. *Geophysical Journal International* **175**, 222–238.
- Polet, J., and H. K. Thio (forthcoming). Rapid characterization of a centroid moment tensor and waveheight predictions around the north Pacific for the 2011 Tohoku earthquake. *Earth, Planets and Space*.
- Tsuiji, S., K. Abe, K. Takano, and Y. Yamanaka (1995). Rapid determination of M_w from broadband P waveforms. *Bulletin of the Seismological Society of America* **85**, 606–613.
- Wald, D. J., K.-W. Lin, and V. Quitoriano (2008). *Quantifying and Qualifying USGS ShakeMap Uncertainty*. USGS Open-File Report 2008-1238, 26 pp.
- Wessel, P., and W. H. F. Smith (1991). Free software helps map and display data. *Eos, Transactions, American Geophysical Union* **72**, 445–446.

*U.S. Geological Survey
National Earthquake Information Center
Golden, Colorado 80401 U.S.A
ghayes@usgs.gov
(G. P. H.)*